Random Mutagenesis of the Poly(ADP-ribose) Polymerase Catalytic Domain Reveals Amino Acids Involved in Polymer Branching†

Véronique Rolli,‡ Minnie O'Farrell,§ Josiane Ménissier-de Murcia,‡ and Gilbert de Murcia*,‡

Ecole Supérieure de Biotechnologie de Strasbourg, UPR A9003 du CNRS, Cancérogenèse et Mutagenèse Moléculaire et Structurale, Boulevard Sébastien Brant, F-67400 Illkirch-Graffenstaden, France, and Department of Biological Sciences, University of Essex, Colchester, England

Received May 6, 1997; Revised Manuscript Received July 15, 1997⊗

ABSTRACT: Poly(ADP-ribose) polymerase (PARP) is a multifunctional nuclear zinc finger protein which participates in the immediate response of mammalian cells exposed to DNA damaging agents. Given the complexity of the poly(ADP-ribosylation) reaction, we developed a large-scale screening procedure in *Escherichia coli* to identify randomly amino acids involved in the various aspects of this mechanism. Random mutations were generated by the polymerase chain reaction in a cDNA sequence covering most of the catalytic domain. Out of 26 individual mutations that diversely inactivated the full-length PARP, 22 were found at conserved positions in the primary structure, and 24 were located in the core domain formed by two β-sheets containing the active site. Most of the PARP mutants were altered in poly(ADP-ribose) elongation and/or branching. The spatial proximity of some residues involved in chain elongation (E988) and branching (Y986) suggests a proximity or a superposition of these two catalytic sites. Other residues affected in branching were located at the surface of the molecule (R847, E923, G972), indicating that protein−protein contacts are necessary for optimal polymer branching. This screening procedure provides a simple and efficient method to explore further the structure−function relationship of the enzyme.

Poly(ADP-ribose) polymerase (PARP,[1] EC 2.4.2.30) is a nuclear zinc-finger enzyme involved in the detection and signaling of DNA strand breaks resulting either from the direct action of genotoxins or as generated during excision repair. In response to these breaks acting as an essential cofactor, PARP catalyzes the covalent attachment of ADP-ribose units from NAD^+ to itself (automodification) and to nuclear DNA-binding proteins such as histones and topoisomerases (heteromodification) (Althaus & Richter, 1987; Lautier *et al.*, 1993). Poly(ADP-ribose) glycohydrolase (PARG) is the principal enzyme responsible for the polymer catabolism [for review see Desnoyers *et al.* (1995)]. *In vivo*, the half-life of poly(ADP-ribose) is in the order of few minutes (Alvarez & Althaus, 1989); therefore, poly(ADP-ribosylation is an immediate, but transient, posttranslational modification of nuclear proteins in response to DNA damaging agents.

PARP (113 kDa) is a multifunctional enzyme containing a N-terminal domain encompassing two zinc-finger motifs which acts as a molecular nick-sensor and a bipartite nuclear location signal, a 22 kDa central region bearing the auto-poly(ADP-ribosylation) sites which serves presumably to regulate PARP−DNA interactions, and a C-terminal 54 kDa catalytic domain involved in the nick-binding dependent poly(ADP-ribose) synthesis [for review see de Murcia and Ménissier-de Murcia (1994)]. This domain, which is the most conserved part of the enzyme, can be further restricted to a 40 kDa C-terminal polypeptide without losing the basal activity (Simonin *et al.*, 1993b). It is responsible for the catalysis of three chemically distinct enzymatic steps required for poly(ADP-ribose) synthesis: (i) the specific attachment of one ADP-ribose unit to a glutamate residue in an acceptor protein (initiation reaction) (Kawaichi *et al.*, 1980), (ii) the characteristic (2′−1″) ribose−ribose glycosidic bond formation (elongation reaction), and (iii) the (2″−1‴) ribose−ribose bond between ADP-ribose units at branching points (Miwa *et al.*, 1979). While the initiation reaction occurs via a distributive manner (Mendoza-Alvarez & Alvarez-Gonzalez, 1993; Kawaichi *et al.*, 1981), the last two steps appear to take place via a processive mechanism (Naegeli *et al.*, 1989).

The nature and the function of poly(ADP-ribose) acceptors are highly suggestive of a role of poly(ADP-ribosylation) both in the modulation of chromatin structure at the vicinity of a DNA break and in cell cycle check points. The importance of PARP, as a multifunctional element of the DNA damage surveillance network, has stimulated an interest in the elucidation of its structure and function. In this respect, the crystallographic structure of the chicken PARP

† This work was supported by the Ligue Nationale Contre le Cancer, by the Association pour la Recherche Contre le Cancer, and by Electricité de France.

* To whom correspondence should be addressed. Phone: (33) 0388 65 53 68. Fax: (33) 0388 65 53 43. E-mail: demurcia@esbs.u-strasbg.fr.

‡ Ecole Supérieure de Biotechnologie de Strasbourg.

§ University of Essex.

⊗ Abstract published in *Advance ACS Abstracts*, September 15, 1997.

[1] Abbreviations: PARP, poly(ADP-ribose) polymerase; PARG, poly(ADP-ribose) glycohydrolase; NAD^+, nicotinamide adenine dinucleotide; SDS−PAGE, sodium dodecyl sulfate−polyacrylamide gel electrophoresis; TLC, thin-layer chromatography; PCR, polymerase chain reaction; PMSF, phenylmethanesulfonyl fluoride; EDTA, ethylenediaminetetraacetate; dNTP, deoxynucleoside triphosphate; TCA, trichloroacetic acid.

S0006-2960(97)01055-6 CCC: $14.00

catalytic domain (40 kDa), involved in the nick-binding-dependent poly(ADP-ribose) synthesis, has been recently solved at 2.4 Å resolution in the presence of the nicotinamide analogue PD 128763 (Ruf *et al.*, 1996). Interestingly, the catalytic site of PARP appeared structurally related to that of ADP-ribosylating toxins; both constitute now a superfamily of ADP-ribosyl transferases.

Parallel to this structural approach, to derive structure−activity information, in this work we have generated by PCR a library of human PARP mutants expressed in *Escherichia coli*, mutated specifically in the catalytic domain. Mutations that inactivated to different extent PARP activity were frequently found at highly conserved positions in the primary structure; most of them were located within the β-domain containing the presumptive catalytic site (Ruf *et al.*, 1996). The majority of the mutants were affected in chain elongation. Moreover, five of them were also affected in chain branching, indicating an interdependence of the two functions.

MATERIALS AND METHODS

Mutagenesis, Library Construction, and Transformation into TGE 900 Cells. A 1 kb *Nco*I−*Dra*III cDNA fragment (nucleotides 2056−3045) encoding the human PARP catalytic domain was mutageneized by PCR performed under standard conditions in 100 μL volume consisting of 200 μM each dNTP, 10 mM Tris-HCl, pH 8.4, 50 mM KCl, 2.5 mM $MgCl_2$, 10% gelatin, 50 ng of pBS(−) SHT plasmid bearing the full-length human PARP sequence (Giner *et al.*, 1992), 5 units of *Taq* polymerase, and 1 μg of each primer (sense primer, ATTAACCCTCACTAAG; reverse primer, AGGCCTGCAGGGGAGGATGGC). The amplified sequence (25 cycles: 95 °C, 2 min; 50 °C, 1 min; 70 °C, 1 min in a minicycler from MJ Research, Inc.) was restricted by *Nco*I and *Dra*III and cloned back into the same sites of the procaryotic expression vector pTG161 PARP (Simonin *et al.*, 1991) giving rise to the library of pTG161 PARP* in which the catalytic domain only (amino acids 686−1014) has been mutagenized (referred as PARP*) (Figure 1A). This vector was used directly for transformation of the *E. coli* TGE900 strain (Courtney *et al.*, 1984).

Colony Screening for the Loss-of-Function PARP Mutants.* Colonies (grown at 28 °C) were replica-plated on LB plates containing 50 μg/mL ampicillin. Nitrocellulose filter lifts were then made, and the filters were laid, cells side up, on LB plates containing ampicillin. Protein expression induction was carried out for 5 h at 37 °C. Then, poly(ADP-ribosylation) and immunoreactivity (using an antibody raised against the second zinc finger of the human PARP) were both measured on these same filters (Figure 1B) as described previously (Simonin *et al.*, 1991). Clones that produced the full-size inactive PARP* were isolated and sequenced in the mutagenized cDNA fragment.

Production and Analysis of Recombinant Proteins. Transformed *E. coli* TGE900 cells were grown for 16 h in LB medium at 28 °C, and protein overproduction was obtained following a temperature shift to 37 °C for 5 h (Courtney *et al.*, 1984). Cells were collected and sonicated; proteins were subsequently separated on a 10% SDS−PAGE (Laemmli, 1970) and analyzed using the combined procedure of activity blot and western blot described by Simonin *et al.* (1991) (Figure 1C).

Determination of PARP Activity. Bacteria from a 5 mL culture were lysed by stirring for 20 min at 4 °C in 1 mL of lysis buffer containing 100 mM Tris-HCl, pH 8.0, 100 mM NaCl, 10 mM β-mercaptoethanol, 1 mM phenylmethanesulfonyl fluoride (PMSF), and 1 mg of lysozyme. Cells were then sonicated using a Vibra-cell 72446 (one 60 s pulse at 180 V). The cell lysate was complemented with 0.2% Tween 20, 0.2% Nonidet P-40, and 0.5 M NaCl, stirred for 20 min, sonicated again, and finally cleared by centrifugation (20000*g*, 20 min). To estimate the amount of PARP mutants in cleared lysates, a standard curve was generated by immunoblotting, using purified PARP from the Sf9 insect cell/baculovirus system (Giner *et al.*, 1992) and a polyclonal antibody raised against the second zinc finger of human PARP (Simonin *et al.*, 1991).

Samples corresponding to 200 ng of wild-type or mutant PARP proteins were incubated for 10 min at 25 °C in assay buffer (100 μL) consisting of 50 mM Tris-HCl, pH 8.0, 4 mM $MgCl_2$, 0.2 mM dithiothreitol, 2 μg/mL total histones, 2 μg/mL DNase I−activated calf thymus DNA, 200 μM NAD^+, and 5 μCi/mL [α-^{32}P]NAD^+. The reaction was stopped by addition of 25 μL of 100% trichloroacetic acid (TCA) and 1% inorganic pyrophosphate, and the acid-insoluble radioactivity was counted (Niedergang *et al.*, 1979).

Polymer Analysis. Samples were incubated as in the standard enzymatic assay described above; the reaction was stopped with 100 μL of 40% ice-cold TCA. The TCA pellet obtained by centrifugation at 12000*g* for 15 min was washed 2 times with 20% TCA and 2 times with diethyl ether and dissolved in 30 μL of 0.1 N NaOH containing 20 mM EDTA. After incubation at 60 °C for 2 h, the solution was neutralized with 0.1 N HCl and loaded on a high resolution 20% polyacrylamide gel [acrylamide/bis(acrylamide) in a ratio of 19:1], 100 mM Tris−borate buffer, pH 8.3, and 2 mM EDTA, according to Alvarez-Gonzalez and Jacobson (1987). Short gels (0.15 × 16 × 14 cm) were used to visualize AMP (product of NaOH treatment of the protein−proximal ADP-ribose), mono(ADP-ribose) and low molecular weight oligo(ADP-ribose) ($n < 10$). Long gels (0.02 × 33 × 40 cm) were used to visualize longer polymers of ADP-ribose ($n > 10$). Electrophoresis was carried out at 200 and 2000 V, respectively, and the gels were autoradiographed.

To evaluate the polymer complexity, the radiolabeled material was hydrolyzed by snake venom phosphodiesterase (Worthington-Freehold) and analyzed by two-dimensional thin-layer chromatography (2D TLC) on cellulose plates (F1440; Schleicher and Schuell, Dassel, Germany) according to the method of Keith *et al.* (1990). The chromatograms were quantified by computerized PhosphorImager (Molecular Dynamics) and ImageQuant software. The average polymer size and the branching frequency were calculated according to the method of Miwa and Sugimura (1982).

RESULTS

In Vitro Random Mutagenesis and Screening for Loss-of-Function PARP Mutants.* To identify functionally essential residues in the human PARP catalytic domain, *in vitro* random mutagenesis was achieved by PCR under standard conditions, using the *Taq* polymerase. The rate of misincorporation essentially due to the absence of the 3′−5′

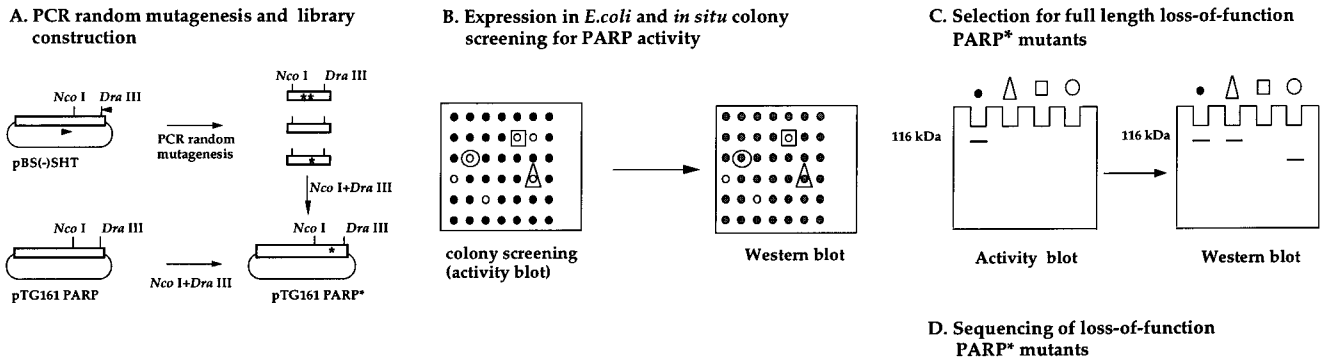

FIGURE 1: Strategy used to generate a library of human PARP catalytic domain mutants. (A) PARP cDNA is indicated by a box in each vector used. Random mutations are represented by asterisks (*) on the plasmid or insert. The primers used for PCR are indicated by two arrows on pBS(−)SHT plasmid. (B) *E. coli* colonies induced to express recombinant human PARP were lifted onto nitrocellulose (see Materials and Methods) and were incubated with [α-^{32}P]NAD$^+$ (activity blot). The same blot was immunostained (Western blot) with anti-PARP antibody to confirm the production of recombinant PARP. Triangles or circles correspond to colonies expressing an inactive enzyme; nonexpressing colonies are indicated by squares. (C) Crude extracts from PARP expressing colonies were separated by a SDS−PAGE, transferred on nitrocellulose, and processed for activity blot followed by a Western blot. The same symbols as in panel B are used: squares correspond to nonexpressing colonies, triangles refer to full-size but inactive PARP, and circles represent truncated inactive PARP.

Table 1: Sequence Analysis and Characterization of PARP Mutants Obtained by Random Mutagenesis of the Human PARP Catalytic Domain

	mutated nucleotide	enzymatic activity (%)	reaction product (gel electrophoresis)	average polymer size (2D TLC)	branching frequency (2D TLC)	branching compared to wild-type
wild type		100	polymer	37.5	0.36	normal
G699R	**G**GG → **A**GG	10	−	30.7	0.19	normal
R704W[a]	**A**GG → **T**GG	40	−	36.3	0.3	normal
L797P	C**T**C → C**C**C	1.5	−	ND		
S808P	**T**CT → **C**CT	20	−	32.3	0.26	normal
R847C	**C**GT → **T**GT	75	−	40	0.28	2× lower
N868S	A**A**C → A**G**C	4	−	ND		
F869S[a]	T**T**T → T**C**T	25	−	23.9	0.18	normal
G871R	**G**GG → **A**GG	17.5	−	35	0.3	normal
L877P	C**T**T → C**C**T	2.5	−	ND		
M890V[a]	**A**CA → **G**CA	<0.5	−	ND		
F897S	T**T**C → T**C**C	10	−	17.8	0.1	normal
F897Y	T**T**C → T**A**C	25	−	28.6	0.21	normal
D899N[a]	**G**AC → **A**AC	0.6	−	ND		
C908R	**T**GC → **C**GC	<0.5	−	ND		
E923G	G**A**A → G**G**A	20	−	48	0.26	3× lower
L926F	**C**TT → **T**TT	1.5	−	ND		
L964P	C**T**G → C**C**G	75	−	37	0.33	normal
G972R	**G**GG → **A**GG	16	−	15.1	0.027	3X lower
L984P[a]	C**T**A → C**C**A	6	−	ND		
Y986H	**T**AT → **C**AT	14	−	14.6	1.15	15X higher
Y986S	T**A**T → T**C**T	11	oligomer	10.8	0.05	normal
E988K[a]	**G**AG → **A**AG	1.25	monomer	ND		
Y989H	**T**AC → **C**AC	65	polymer	38.6	0.36	normal
L999P	C**T**G → C**C**G	30	−	42	0.25	2X lower
Y1001C	T**A**T → T**G**T	13	−	27.6	0.24	normal
L1003P	C**T**G → C**C**G	1.5	−	ND		

[a] Mutants obtained by subcloning of double mutants. Enzymatic assays were performed as described in Materials and Methods. Enzymatic activities are expressed as percentages relative to the wild type (100%) and estimated using values from two to five experiments. The average polymer size and branching frequency were calculated according to Miwa and Sugimura (1982) from 2D TLC results which were similar when repeated. The branching frequency values were compared to the plot of polymer lengths versus number of branching points established by Keith *et al.* (1990) for the wild-type synthezized polymer. ND, not determined.

exonuclease activity of the *Taq* polymerase ranges from 0.1 to 2 per 1000 nucleotides (Tindall & Kunkel, 1988; Eckert & Kunkel, 1991; Spee *et al.*, 1993). The difference between these frequencies is due to the reaction conditions (number of PCR cycles, $MgCl_2$ concentration) but also to the sequence of the amplified DNA (Eckert & Kunkel, 1991). Therefore, the PCR procedure essentially induces transitions (GC to AT and mainly AT to GC), a few deletions, insertions, and transversions.

PARP* mutants specifically mutated in their catalytic domain and expressed in *E. coli* TGE900 were obtained by a two-step selection procedure involving (i) the selection of colonies presenting a total or a partial loss of catalytic activity as detected by the *in situ* colony screening assay (Simonin *et al.*, 1991) and (ii) the size determination of the mutated proteins by western blotting (Figure 1). Therefore, only full-length inactive PARP* mutants were selected for sequencing. Twenty six inactive or partially active human PARP* mutants, with a single base substitution, were finally selected (Table 1). The residual catalytic activity of the mutants expressed in *E. coli* TGE900 was confirmed in cleared lysates (Table 1) under the optimal *in vitro* conditions (18 nM PARP; 200 μM NAD$^+$) defined by Mendoza-Alvarez and Alvarez-Gonzalez (1993).

FIGURE 2: Distribution of the mutations altering the poly(ADP-ribosylation) function on the primary and secondary structures of the human PARP catalytic domain. The randomly mutagenized sequence starts at codon 686 (*Nco*I site) and ends at the stop codon 1015. Amino acid substitutions obtained by random mutagenesis are indicated in bold, above the wild-type human PARP sequence (Uchida *et al.*, 1987). Inactivating mutations obtained by site-directed mutagenesis (Simonin *et al.*, 1990, 1993a) are indicated in italic. Residues photolabeled by 2′-azido-NAD (K893, W1014) (Kim *et al.*, 1997) are circled. The human PARP primary structure has been superposed onto a schematic representation of the secondary structure of the chicken PARP catalytic domain [taken from Ruf *et al.*, (1996)]: α-helices (*A* to *L*) are represented by boxes and *β*-strands (*a* to *n*) as arrows. The shadowed box (residues 859−908) represents the most conserved region of PARP. The amino acids structurally conserved and homologous to those contacting directly NAD^+ in DT (Bell & Eisenberg, 1996) are underlined. F* corresponds to the gain-of-function mutation (L713F) (Alves Miranda *et al.*, 1995).

Amino Acid Substitutions. The rate of PARP* mutants as expressed by the ratio of inactive mutated colonies over colonies expressing an active PARP* was 2%. Twenty-six point mutants were obtained; in most cases the sequenced substitutions were transitions leading to a missense mutation at the amino acid level (Table 1). Six among 26 inactive mutants initially contained a double substitution; each of them was individually examined following a subcloning procedure which gave six single point mutated inactive PARP* (Table 1) and six noncontributing mutations: Q722H, S724G, N820D, H909R, H937R, and A995V. Four nonsense mutations were also obtained leading to C-terminal truncated inactive mutants, Δ973−1014, Δ994−1014, Δ996−1014, and Δ999−1014, thus confirming the inability of the extreme C-terminal region to tolerate even short deletions (Simonin *et al.*, 1990; Kim *et al.*, 1997). Interestingly, the insertion of two amino acids (Thr-Tyr) at position 987 also inactivated the recombinant PARP, further demonstrating the importance of this region for catalysis.

The distribution of single amino acid substitutions, inactivating PARP to various extents, is displayed with respect to the primary and the secondary structures of the human PARP catalytic domain (Figure 2) as taken from the crystal structure of the chicken enzyme (Ruf *et al.*, 1996). A

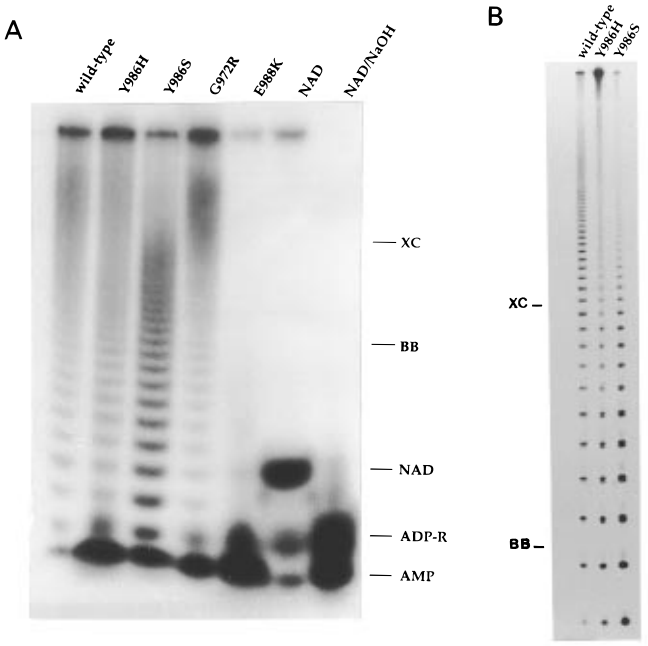

FIGURE 3: Size distribution of ADP-ribose polymers synthesized by wild-type PARP and PARP* mutants. Assays (100 μL) containing 18 nM recombinant PARP protein and 200 μM [α-^{32}P]-NAD^+ were incubated 10 min at 25 °C. The protein-bound ADP-ribosylation products were released by 0.1 N NaOH and 20 mM EDTA. Neutralized samples were run on a 20% polyacrylamide gel. The same amount of Cerenkov counts was loaded for the wild-type and each PARP* mutant. Panel A: short-size polymer analysis. Some hydrolysis of ADP-ribose to form AMP occurred during treatment with alkali. NaOH-treated [α-^{32}P]NAD^+ was loaded to visualize the adenosine derivatives, ADP-ribose and AMP. Panel B: long-size polymer analysis. The electrophoretic mobilities of xylene cyanol (XC) and bromophenol blue (BB) are shown for reference.

nonrandom distribution of substitutions can be clearly observed: (i) most of the mutations (24/26) fall in the core domain formed by two *β*-sheets (residues 785−1010) containing the putative active site; (ii) 9/26 substitutions were found located at the most conserved region of the enzyme (residues 859−908) (de Murcia & Ménissier-de Murcia, 1994; Lepiniec *et al.*, 1995) now considered as the "PARP signature" and containing the amino acids homologous to those involved in NAD^+ binding in diphtheria toxin (DT) (Bell & Eisenberg, 1996; Ruf *et al.*, 1996); (iii) 5/26 were located at or near the site of glutamic acid 988, an essential residue for polymer formation (Marsischky *et al.*, 1995). It is also interesting to note the occurrence of the Leu → Pro mutations (6/26) due to the preference of the *Taq* polymerase for inducing T → C transitions (Tindall & Kunkel, 1988), resulting probably in dramatic structural changes.

Quantitative and Qualitative Analysis of the Reaction Products. To characterize the reaction product of the PARP* mutants, the radiolabeled material synthesized in the presence of [α-^{32}P]NAD^+ was removed from the acceptor proteins by alkali treatment and fractionated by electrophoresis on short (Figure 3A) or long (Figure 3B) 20% polyacrylamide gels. In contrast to the wild-type enzyme which synthesized high molecular weight polymers, most of the mutants were affected in chain elongation as indicated both by the accumulation of AMP produced during the degradation by NaOH of the protein−proximal ADP-ribose (Hilz & Stone, 1976) and by the amount of synthesized mono-(ADP-ribose) (Figure 3A). This effect is marked for the

mutant G972R and more dramatically for E988K, which catalyzed exclusively the mono(ADP-ribosylation) reaction, a result in full agreement with the work of Marsischky *et al.* (1995) demonstrating the necessity to have a side chain carboxylate at this precise spatial location to ensure polymer elongation activity.

Codon 986 was mutated twice, giving the mutants Y986S and Y986H. The mutant Y986S, also affected in chain elongation, produced mainly oligomers of ADP-ribose (Figure 3A), whereas the mutant Y986H synthesized both low and (apparently) high molecular weight material. This particular distribution of ADP-ribose polymers was better visualized using long polyacrylamide gels. Figure 3B shows again the predominant synthesis of oligomers associated with the substitution Y986S, whereas in the case of Y986H, the accumulation of high molecular weight material on the top of the gel as well as a smear (for $n > 20$) was clearly observed.

The reaction products were further characterized by 2D TLC following polymer hydrolysis by snake venom phosphodiesterase according to Keith *et al.* (1990). Measurements of label in phosphoribosyl-AMP (PRAMP, main chain product), AMP (present at the polymer termini), and diphosphoribosyl-AMP (PR_2AMP, found at the branching points) provided the basis for polymer size, chain length, and branching frequency calculations (Miwa & Sugimura, 1982). Due to the low amount of incorporated radioactivity, mutants displaying less than 10% of the wild-type enzymatic activity were not analyzed. The results summarized in Table 1 indicate that most of the PARP* mutants synthesized polymers of ADP-ribose with various efficiency, but with the same branching frequency as the wild-type; the variation of branching frequency as a function of the polymer size being taken from Keith *et al.* (1990). However, in five cases, a loss- (R847C, E923G, G972R, L999P) or a gain-of-function (Y986H) in terms of branching frequency was detected. Representative chromatograms corresponding to the amino acid substitutions at positions 972 and 986 are shown in Figure 4. Compared to the wild-type PARP treated under the same experimental conditions, the relative amount of PR_2AMP is normal for the mutant Y986S, decreased for the mutant G972R, but dramatically increased for the mutant Y986H. Therefore, the presence of a smear observed for polymers longer than 20 ADP-ribose units (Figure 3B) and the accumulation of highly branched polymers at the top of the 20% acrylamide gels (Figure 3B) together with the very high proportion of PR_2AMP detected by 2D TLC (Figure 4) strongly argue for a critical role of the amino acid Y986 in the elongation and/or the branching reaction of poly(ADP-ribose).

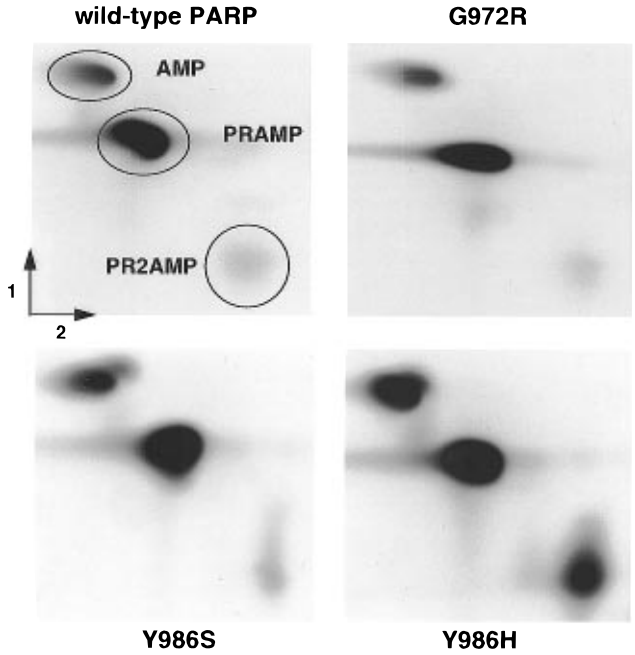

FIGURE 4: Thin-layer chromatography on venom phosphodiesterase-hydrolyzed polymers of ADP-ribose synthesized by the wild-type and PARP* mutants. Wild-type and PARP* mutants (200 ng) were incubated under the standard conditions for 10 min at 25 °C. Radiolabeled ADP-ribose polymers were hydrolyzed with snake venom phosphodiesterase, and the polymer constituents obtained were analyzed by 2D TLC (see Materials and Methods). Abbreviations: PRAMP, phosphoribosyl-AMP; $(PR)_2AMP$, diphosphoribosyl-AMP.

DISCUSSION

The goal of an analysis of structure−function relationships in a protein is to specify how different parts of the polypeptide give rise to the form and function of the molecule. Deletion experiments (Simonin *et al.*, 1990; Cherney *et al.*, 1991), site-directed mutagenesis (Simonin *et al.*, 1993a; Marsischky *et al.*, 1995), and photolabeling (Kim *et al.*, 1997) have given complementary information to identify regions and residues that are important for catalytic activity of PARP. To pinpoint unexpected residues involved in the complex mechanism of the poly(ADP-ribosylation) reaction, in this study we have generated a random library of PARP mutants affected in the catalytic domain. Using this technique, mutations affecting the catalytic activity but not its DNA binding capacity were identified recently in the amino-terminal domain of PARP (Trucco *et al.*, 1996). The chief advantages of this procedure, compared to other methods, are its technical simplicity and its potential capacity to screen both for rescue mutations (using a PCR library of cDNA encoding inactive PARPs) and for gain-of-function mutations. Such an engineered PARP mutant (L713F) affected in the k_{cat} value (9-fold increase) but not in the Michaelis constant for NAD^+ was isolated by the same procedure (Alves Miranda *et al.*, 1995).

Out of the 26 missense point mutations characterized, 22 occurred at conserved positions in a multiple alignment of PARP sequences from human to *Arabidopsis thaliana* (Lepiniec *et al.*, 1995). The crystal structure of the chicken PARP catalytic domain has been recently solved at 2.4 Å resolution in the presence or in the absence of the nicotinamide analogue PD128763 (3,4-dihydro-5-methylisoquinolinone; Parke-Davis) (Ruf *et al.*, 1996). It is composed of two parts: (i) an N-terminal region formed by a bundle of six α-helices (*A*−*F* in Figure 2; residues 662−784) and (ii) a C-terminal region made of two *β*-sheets surrounded by five α-helices (residues 785−1014) containing the presumptive NAD^+-binding cavity suggested by the presence of the inhibitor PD128763 in the cocrystal. This C-terminal part includes a highly conserved block of 50 amino acids (residues 859−908) folded in a *β*−α-loop-*β*−α motif structurally similar to the NAD^+-binding fold of mono(ADP-ribosylating) toxins like diphtheria toxin (DT) (Bell & Eisenberg, 1996), exotoxin A from *Pseudomonas aeruginosa* (ETA) (Li *et al.*, 1996), pertussis toxin (PT) (Stein *et al.*, 1994), cholera toxin

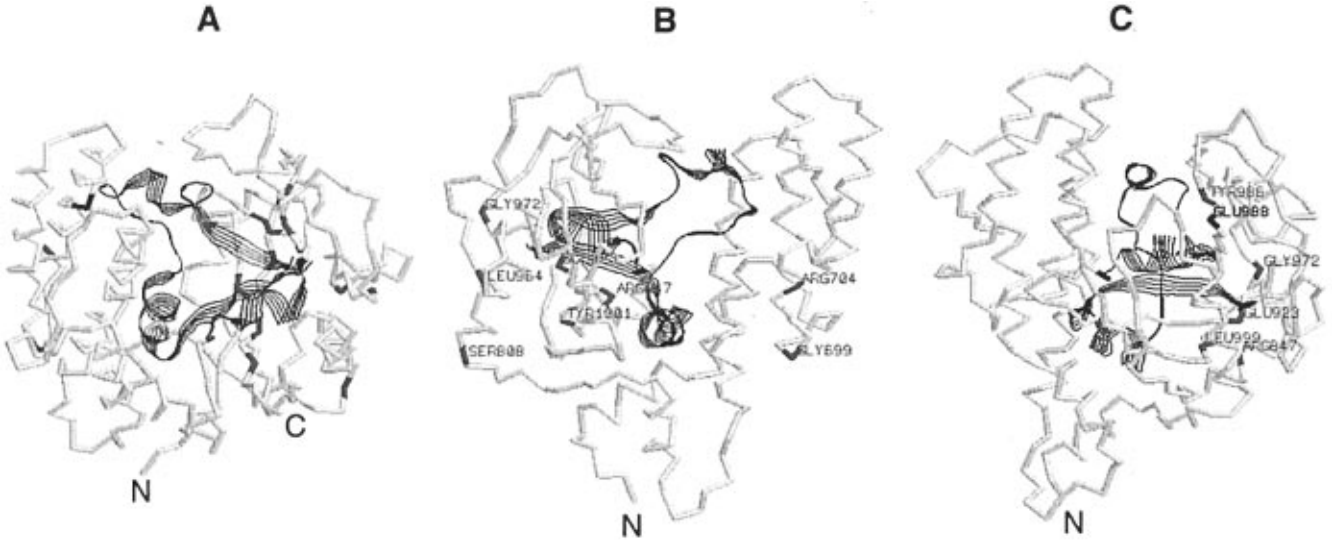

FIGURE 5: Distribution of the mutations inactivating the ADP-ribosylation reactions on the crystal structure of the chicken PARP catalytic fragment [taken from Ruf *et al.* (1996), residues 662−1010, human numbering]: (A and C) front view of the C^{α} backbone; (B) back side of the molecule. The block of conserved residues (859−908) is indicated by a black ribbon. Panel A represents the 26 residues (in red) hit by random mutagenesis and affecting PARP activity. The gain-of-function mutant L713F is shown in green. Panel B represents mutated residues located at the surface of the catalytic fragment. Panel C shows the amino acids (in red) involved in polymer branching. The active site glutamate E988 is shown in blue.

(CT) (Zhang *et al.*, 1995), and heat-labile enterotoxin (LT) (Sixma *et al*., 1991). As displayed in Figure 5A, 35% (9/26) of the inactivating substitutions obtained by random mutagenesis are located in the crevice delineated by the motif $\beta-\alpha$-loop-$\beta-\alpha$, thus confirming the importance of this supersecondary structure in NAD^+ binding and/or catalysis (Ruf *et al.*, 1996; Kim *et al*., 1997).

Many of the mutations may affect the thermodynamic stability of the mutated enzyme by disrupting the hydrophobic core of the enzyme (*i.e.*, L797P, C908R, L926F, L1003P). The implication of proline in protein flexibility and therefore activity could also explain the occurrence of the Leu → Pro mutations (6/26). Some other mutations have a location in the crystal structure which is suggestive of a role in catalytic activity. First, the α-helical domain (residues 662−784) absent in ADP-ribosylating toxins appears to be specific for poly(ADP-ribose) synthesis. This region, lining the active site pocket with helix F (Figure 5A), has been suggested to relay the activation signal issued on binding to damaged DNA, giving rise presumably to a more favorable NAD^+-binding mode (Ruf *et al.*, 1996). It is worth mentioning that a major change of mobility of the active site loop has been observed in ETA (Li *et al*., 1995) and DT (Bell & Eisenberg, 1996), supposedly favoring the binding of the acceptor substrate EF-2 following NAD^+ binding. In PARP, the gain-of-function mutation L713F located in helix D, 7.1 Å from the active site loop (Figures 2 and 5A), was shown to increase the catalytic constant by a factor of 9 (Alves Miranda *et al*., 1995), suggesting that, similarly, a loop movement may have been induced by this substitution, increasing presumably the access of the cleft to the substrate.

Conversely, the substitutions G699R and R704W located at the surface of the α-helical domain (Figure 5B) decrease the catalytic activity, indirectly perhaps, through a modification of inter- or intramolecular contacts by altering the surface charge. Second, some of the mutations affecting the branching function (R847C, E923G, G972R) are located in the external face of the catalytic fragment (Figure 5B). These residues, together with Y986H and L999P (Figure 5C) also affected in branching, are not close enough to constitute a site for branching; they may form an additional interface region for protein−protein contacts required for optimal polymer branching. The same is true for the substitutions at positions 808, 964, and 1001 which are also located in the external face but are affected in chain elongation. Noncontributing residues (see Results) were found to be localized at the surface of the protein, out of the two regions defined above comprising residues G699 and R704 in the α-helical domain or S808, R847, G923, L964, G972, and Y1001 respectively (Figure 5B). Interestingly, all of these residues are absent in ADP-ribosylating toxins, suggesting that they participate to an additional mecanism to catalyze elongation and branching of poly(ADP-ribose).

The majority of the PARP* mutants that we have characterized are altered in the ratio initiation/elongation as demonstrated by an accumulation of the first ADP-ribose residue (Figure 3A). Only one mutant (Y986S) presented a size-limited synthesis of ADP-ribose oligomers as shown in Figure 3B. However, complete loss-of-function mutants (*i.e.*, affected in the initiation reaction) were never obtained. E988K, located near the NAD^+-binding pocket, was by far the most severe mutation obtained, demonstrating a crucial role of this highly conserved residue in catalysis of polymer elongation (Marsischky *et al.*, 1995). The remarkable conservation of the nicotinamide subsite in PARP, DT, ETA, and PT and the similar spatial location of their respective active site glutamate are suggestive of a common mechanism. For bacterial ADP-ribosylating toxins it has been proposed to proceed via an S_N1 attack, leaving a positively charged oxocarbonium intermediate stabilized by the essential glutamate, the ADP-ribose being docked in the NAD^+ cavity until it is transferred to the acceptor. A S_N2 displacement mechanism has been proposed also with nucleophilic attack on NAD^+ by an incoming nucleophile (the diphthamide moiety of EF-2 in the case of DT) activated by the glutamate residue acting as a general base. In PARP, the substitution at position E988 has no effect on NAD^+ binding (Marsischky

et al., 1995), but it strongly affects chain elongation, a transfer reaction in which the newly produced ADP-ribose is linked to the 2′-OH of the adenine ribose, at the distal end of the growing polymer. It is likely that a similar mechanism of ADP-ribose transfer exists in PARP and bacterial toxins in which a glutamate residue located strictly at the same spatial position in the NAD^+-binding cavity, 4 Å from the anomeric C1′N atom of the nicotinamide ribose (Bell & Eisenberg, 1996), activates and/or stabilizes the incoming ADP-ribose acceptor substrate for chain elongation.

Interestingly, the substitution at position Y986, close to the glutamate active site, increased dramatically the branching frequency (15-fold), suggesting either a close proximity of the elongation and the branching sites or a dependence of the periodic occurrence of branching points (every 40 ADP-ribose units; Keith *et al*., 1990), upon the correct progression of the elongation reaction. During polymer synthesis, the ADP-ribose acceptor site is switched from the 2′-OH of the adenine ribose in linear portions to the 2′-OH of the ribose relative to the nicotinamide to initiate regular branching points; in both cases, however, the same α(1→2) linkage is catalyzed (Miwa *et al.*, 1981). The capacity of the mutant Y986H to produce highly branched but short polymers of an average chain length of 4.4 units (Table 1) indicates that the branching function of PARP is not dependent upon a given polymer size, permitting enough flexibility of the linear chain for a switch of ribose at regular intervals. A steric hindrance between two facing PARP molecules acting in an intermolecular reaction cannot be also invoked to explain the branching periodicity since very short distances can separate two successive branches (Table 1). This intriguing property of PARP to catalyze branched poly(ADP-ribose) could be due to the intrinsic helical nature of this polymer (Minaga & Kun, 1983), allowing a better accessibility of the nicotinamide ribose after a linear synthesis of 40 units. In that case, the substitution Y986H would introduce enough distortion at the polymer termini to expose this "wrong" ribose for chain elongation.

The branched nature of the polymer has been evoked to explain the selective electrostatic binding of histones in an *in vitro* shuttle mechanism leading to chromatin depletion following DNA damage (Realini & Althaus, 1992; Althaus *et al.*, 1995). The possibility of transfecting constructs expressing some of the PARP mutants described in this study, in PARP-deficient cell lines obtained by homologous recombination (Ménissier-de Murcia *et al*., 1997), opens new lines of investigation to further explore *in vivo* the structure−function relationship of poly(ADP-ribose).

ACKNOWLEDGMENT

We are indebted to Dr. R. Alvarez-Gonzalez for his help in polymer analysis, to Drs. G. Keith and F. Schuber for critical reading of the manuscript, and to A. Ruf and Dr. G. E. Schulz for helpful discussions.

REFERENCES

Althaus, F. R., & Richter, C. (1987) *Mol. Biol. Biochem. Biophys. 37*, 1−126.

Althaus, F. R., Bachmann, S., Höfferer, L., Kleczkowska, H. E., Malanga, M., Panzeter, P., Realini, C., & Zweifel, B. (1995) *Biochimie 77*, 423−432.

Alvarez Gonzalez, R., & Jacobson, M. K. (1987) *Biochemistry 26*, 21907−21913.

Alvarez Gonzalez, R., & Althaus, F. R. (1989) *Mutat. Res. 218*, 67−77.

Alves Miranda, E., Dantzer, F., O'Farrell, M., de Murcia, G., & Ménissier-de Murcia (1995) *Biochem. Biophys. Res. Commun. 212*, 317−325.

Bell, C. E., & Eisenberg, D. (1996) *Biochemistry 35*, 1137−1149.

Cherney,B., Chaudry, B., Bhatia, K., Butt, T. R., & Smulson, M. (1991) *Biochemistry 30*, 10420−10427.

Courtney, M., Buchwalder, A., Tessier, L. H., Jaye, M., Benavente, A., Balland, A., Kohli, V., Lathe, R., Tolstoshev, P., & Lecocq, J. P. (1984) *Proc. Natl. Acad. Sci. U.S.A. 81*, 669−673.

de Murcia, G., & Ménissier de Murcia, J. (1994) *Trends Biochem. Sci. 19*, 172−176.

Desnoyers, S., Shah, G. M., Brochu, G., Hoflack, J. C., Verreault, A., & Poirier, G. G. (1995) *Biochimie 77*, 433−438.

Eckert, K. A., & Kunkel, T. A. (1991) *PCR Methods Appl. 1*, 17−24.

Giner, H., Simonin, F., de Murcia, G., & Ménissier-de Murcia, J. (1992) *Gene 114*, 279−283.

Hilz, H., & Stone, P. R. (1976) *Rev. Physiol. Biochem. Pharmacol. 76*, 1−58.

Kawaichi, M., Ueda, K., Hayaichi, O. (1980) *J. Biol. Chem. 255*, 816−819.

Kawaichi, M., Ueda, K., Hayaichi, O. (1981) *J. Biol. Chem. 256*, 9483−9589

Keith, G., Desgrès, J., & de Murcia, G. (1990) *Anal. Biochem. 191*, 309−313.

Kim, H., Jacobson, M. K., Rolli, V., Ménissier-de Murcia, J., Reinbolt, J., Simonin, F., Ruf, A., Schulz, G. E., & de Murcia, G. (1997) *Biochem. J. 322*, 469−475.

Laemmli, U. K. (1970) *Nature 227*, 680−685.

Lautier, D., Lagueux, J., Thibodeau, J., Ménard, L., & Poirier, G. (1993) *Mol. Cell. Biochem. 122*, 171−193.

Lepiniec, L., Babiychuk, E., Kushnir, S., Van Montagu, M., & Inzé, D. (1995) *FEBS Lett. 364*, 103−108.

Li, M., Benhar, I., Pastan, I., & Davies, R. D. (1995) *Proc. Natl. Acad. Sci. U.S.A. 92*, 9308−9312.

Marsischky, G. T., Wilson, B., & Collier, R. J. (1995) *J. Biol. Chem. 270*, 3247−3254.

Mendoza-Alvarez, H., & Alvarez-Gonzales, R. (1993) *J. Biol. Chem. 268*, 22575−22580.

Ménissier-de Murcia, J., Niedergang, C., Trucco, C., Ricoul, M., Dutrillaux, B., Mark, M., Oliver, J., Masson, M., Dierich, A., LeMeur, M., Balzinger, C., Chambon, P., de Murcia, G. (1997) *Proc. Natl. Acad. Sci. U.S.A. 94*, 7303−7307.

Minaga, T., & Kun E. (1993) *J. Biol. Chem. 258*, 725−730.

Miwa, M., & Sugimura, T. (1982) in *ADP-Ribosylation Reactions, Biology and Medicine* (Hayaishi, O., & Ueda, K., Eds.) pp 43−62, Academic, New York.

Miwa, M., Saikawa, N., Yamaizumi, Z., Nishimura, S., & Sugimura, T. (1979) *Proc. Natl. Acad. Sci. U.S.A. 76*, 595−599.

Miwa, M., Ishihara, M., Takishima, S., Takasuka, N., Maeda, M., Yamaizumi, Z., & Sugimura, T. (1981) *J. Biol. Chem. 256*, 2916−2921.

Naegeli, H., Loetscher, P., & Althaus, F. R. (1989) *J. Biol. Chem. 264*, 14382−13484.

Niedergang, C., Okazaki, H., & Mandel P. (1979) *Eur. J. Biochem. 102*, 43−57.

Realini, C. A., Althaus, F. R. (1992) *J. Biol. Chem. 267*, 18858−18865.

Ruf, A., Ménissier-de Murcia, J., de Murcia, G., & Schulz, G. E. (1996) *Proc. Natl. Acad. Sci. U.S.A. 93*, 7481−7485.

Simonin, F., Ménissier-de Murcia, J., Poch, O., Muller, S., Gradwohl, G., Molinete, M., Penning, C., Keith, G., & de Murcia, G. (1990) *J. Biol. Chem. 265*, 19249−19256.

Simonin, F., Briand, J. P., Muller, S., & de Murcia, G. (1991) *Anal. Biochem. 195*, 226−231.

Simonin, F., Poch, O., Delarue, M., & de Murcia, G. (1993a) *J. Biol. Chem. 268*, 8529−8535.

Simonin, F., Höfferer, L., Panzeter, P., Muller, S., de Murcia, G., & Althaus, F. (1993b) *J. Biol. Chem*. 268, 13454−13461.

Sixma, T. K., Pronk, S. E., Kalk, K. H., Wartna, E. S., van Zanten, B. A. M., Witholt, B., & Hol, W. G. J. (1991) *Nature 351*, 371−377.

Spee, J. H., de Vos, W. M., & Kuipers, O. P. (1993) *Nucleic Acids Res. 21,* 777−778.
Stein, P. E., Boodhoo, A., Armstrong, G. D., Cockle, S. A., Klein, M. H., & Read, R. J. (1994) *Structure 2,* 45−57.
Tindall, K. R., & Kunkel, T. A. (1988) *Biochemistry 27,* 6008−6013.
Trucco, C., Flatter, E., Fribourg, S., de Murcia, G., & Ménissier-de Murcia, J. (1996) *FEBS Lett. 399,* 313−316.
Uchida, K., Morita, T., Sato, T., Ogura, T., Yamashita, R., Nogushi, S., Suzuki, H., Nyunoya, H., Miwa, M., & Sugimura, T. (1987) *Biochem. Biophys. Res. Commun. 148,* 617−622.
Zhang, R. G., Scott, D. L., Westbrook, M. L., Nance, S., Spangler, B. D., Shipley, G. G., Westbrook, E. M. (1995) *J. Mol. Biol. 251,* 563−573.

BI971055P